

IDENTIFYING SENSITIVE PARAMETERS AT FATIGUE CRACK NUCLEATION SITES USING MICROSTRUCTURAL SIMULATION MODELS

Robert G. Tryon¹, Animesh Dey¹, Ganapathi Krishnan¹, K. S. Ravi Chandran², Michael Oja²

¹VEXTEC Corporation, 750 Old Hickory Blvd, Bldg. 2 Suite 270, Brentwood, TN 37027, USA

²Department of Metallurgical Engineering, University of Utah, 135 S 1460 E Rm. 412, Salt Lake City, UT 84112, USA

Keywords: fatigue, probabilistic, nickel, prognosis, Waspaloy

Abstract

High strength components exposed to cyclic loading such as gas turbine disks fail in an insidious manner, giving no prior indication that damage has occurred. Cracking takes place on a very small scale and the critical damage state is reached when the crack is very small. Unfortunately, cracks of these sizes are difficult to detect. Often, long crack damage is considered when performing fatigue diagnostics. However, an accurate onboard prognostic capability should consider total life as initiation and long crack growth. Prognostication of small cracks requires simulating fatigue damage accumulation from the evolution of micro scale damage initiation. This paper discusses methods for predicting the probability of fatigue failure from cracks starting on the micro scale. These methods predict the variation in fatigue life based on the statistical variation in the microstructure of the material. Material parameters at the metallic grain level are integrated with fundamental physics-based models to predict the damage as it accumulates.

Introduction

Diagnosis and prognosis of fatigue damage in metallic materials requires an understanding of the conditions that are likely to lead to fatigue failure. These conditions include temperatures, mechanical loads, dwell times and the material resistance. Fatigue failures in highly stressed high strength components can occur when the critical damage size is very small. Failure often occurs before any damage can be diagnosed with conventional methods. This paper discusses a methodology to aid in the diagnosis and prognosis of metallic components using probabilistic microstructural fatigue models. The capabilities are aimed at simulating the fatigue process from the earliest stage and identifying the microstructural conditions that are likely to exist at the location of fatigue damage initiation. Material parameters at the metallic grain level are used along with fundamental physics-based models to predict the damage as it accumulates. The methods use a virtual prototyping technique relying on computer simulation of real material behavior. The computer simulates many statistically “identical” components but uses a different but statistically equivalent material microstructure for each simulation. The microstructure of each simulated component is properly sampled from the specified range of material parameters. Each of the components is then virtually tested using computer models to simulate real-world usage conditions. The virtual testing allows the “gathering” of data on thousands of components.

Fatigue damage of polycrystalline metallic materials usually begins on a very small scale. Damage initiation is often caused by the irreversible dislocations of atoms within grains or around sub-

grain size defects at or near the specimen surface. The damage culminates in slip bands or microcracks. Purely empirical methods to study damage initiation are difficult because it is almost impossible to determine where the damage will begin. Early fatigue damage is often visible through microscopic observation of the specimen surface. However, the limited field of view of the microscope requires laborious scans of the specimen surface and even then, the damage is often well beyond the nucleation stage before the damage is large enough to be distinguished from other microstructural features.

One aspect of materials prognosis is to access the fatigue resistance of a component prior to the component being placed in service. If conditions that are sympathetic to fatigue failure can be determined, then these conditions can be measured and a determination of fatigue resistance can be made. In this paper, the fatigue response of a nickel alloy is simulated and the microstructural conditions that lead to the initiation of the fatigue failure are determined. By comparing the failure causing microstructural conditions of many simulated components, the significance of the microstructural variable is accessed. This allows for the determination of which microstructural variable need to be measured to determine the fatigue resistance. The predicted conditions at the crack initiation site are then compared with conditions observed from laboratory fatigue test of Waspaloy specimens.

Probabilistic Microstructural Fatigue Model

Figure 1 shows the three levels of damage accumulation that are assumed in the present study. First, the crack nucleates on a small scale on the order of the grain size. Then the crack grows as a microstructurally small crack in which the crack front lies in relatively few grains. The material properties averaged along the crack front, approach bulk material properties as the crack grows and the number of grains interrogated by the crack front increase. At this point, linear elasticity can be assumed and the crack grows as a typical long crack until final failure.

The models used to predict the behavior for each of the three levels of damage accumulation have been discussed elsewhere (Tryon, 1997) and are overviewed below.

Crack Nucleation Model

The crack nucleation model assumes slip band cracking within a grain. The model is based on a work by Tanaka and Mura (1981) and extended to account for grain orientation by Tryon and Cruse (1998) as

Report Documentation Page

Form Approved
OMB No. 0704-0188

Public reporting burden for the collection of information is estimated to average 1 hour per response, including the time for reviewing instructions, searching existing data sources, gathering and maintaining the data needed, and completing and reviewing the collection of information. Send comments regarding this burden estimate or any other aspect of this collection of information, including suggestions for reducing this burden, to Washington Headquarters Services, Directorate for Information Operations and Reports, 1215 Jefferson Davis Highway, Suite 1204, Arlington VA 22202-4302. Respondents should be aware that notwithstanding any other provision of law, no person shall be subject to a penalty for failing to comply with a collection of information if it does not display a currently valid OMB control number.

1. REPORT DATE 2006		2. REPORT TYPE		3. DATES COVERED 00-00-2006 to 00-00-2006	
4. TITLE AND SUBTITLE identifying Sensitive Parameters at Fatigue Crack nucleation Sites Using Microstructural Simulation Models				5a. CONTRACT NUMBER	
				5b. GRANT NUMBER	
				5c. PROGRAM ELEMENT NUMBER	
6. AUTHOR(S)				5d. PROJECT NUMBER	
				5e. TASK NUMBER	
				5f. WORK UNIT NUMBER	
7. PERFORMING ORGANIZATION NAME(S) AND ADDRESS(ES) VEXTEC Corporation,750 Old Hickory Blvd Bldg 2 Suite 270,Brentwood,TN,37027				8. PERFORMING ORGANIZATION REPORT NUMBER	
9. SPONSORING/MONITORING AGENCY NAME(S) AND ADDRESS(ES)				10. SPONSOR/MONITOR'S ACRONYM(S)	
				11. SPONSOR/MONITOR'S REPORT NUMBER(S)	
12. DISTRIBUTION/AVAILABILITY STATEMENT Approved for public release; distribution unlimited					
13. SUPPLEMENTARY NOTES The original document contains color images.					
14. ABSTRACT see report					
15. SUBJECT TERMS					
16. SECURITY CLASSIFICATION OF:			17. LIMITATION OF ABSTRACT	18. NUMBER OF PAGES 8	19a. NAME OF RESPONSIBLE PERSON
a. REPORT unclassified	b. ABSTRACT unclassified	c. THIS PAGE unclassified			

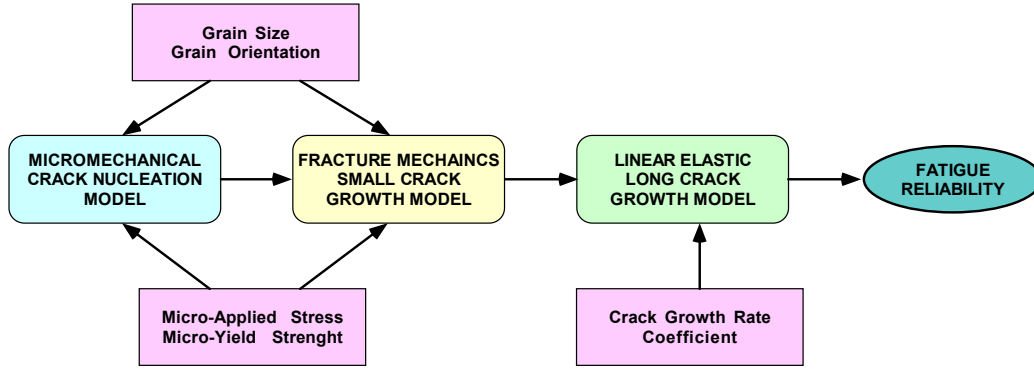


Figure 1 Three-stage micromechanical fatigue model

$$N_n = \frac{4GW_s}{\left(\frac{1}{M_s}\Delta\sigma - 2k\right)^2 \pi(1-\nu)d} \quad (1)$$

where N_n is the number of cycles needed to grow a crack to the size of the grain, G is the shear modulus, W_s is the specific fracture energy per unit area, σ is the local applied normal stress, M_s is grain orientation factor (reciprocal Schmid factor), k is the frictional stress which must be overcome to move dislocations, ν is Poisons ratio, and d is the grain diameter.

Small Crack Growth Model

The experimentally observable parameter that has been correlated to small crack growth rate is the crack tip opening displacement (CTOD) [6]

$$\frac{da}{dN} = C'\Delta\phi_i \quad (2)$$

where a is the crack length, N is cycles, ϕ_i is the CTOD, and C' is a material constants derived from test data. The CTOD is a measure of the amount of damage associated with the crack tip. The larger the CTOD, the higher the crack growth rate.

In the current paper, the CTOD is modeled as an analytical function of the random microstructural variables based on the approach used by Tanaka et al. (1992) and extended by Tryon (1997). Consider a crack of length a with the crack tip in the j^{th} grain as shown in Figure 2. The slip band has a length of w with the slip band tip in the n^{th} grain. The total length of the damage, c , is the crack length plus the slip band length. The size of the slip band zone can be found from

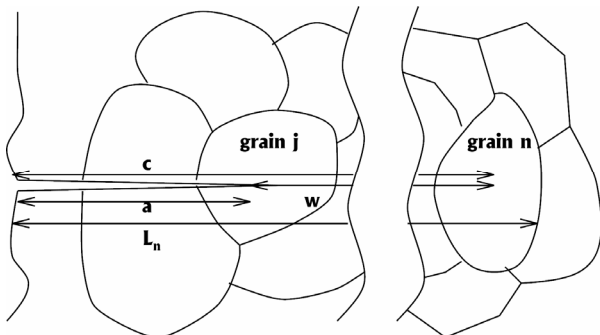


Figure 2: Crack tip slip band in multiple grains

$$0 = \frac{\pi\tau_j}{2} - k_j \arcsin \frac{a}{c} - \sum_{i=j+1}^n [(\tau_{i-1} - k_{i-1}) - (\tau_i - k_i)] \arcsin \left(\frac{L_{i-1}}{c} \right) \quad (3)$$

where, τ_i is the applied resolved shear stress in the i^{th} grain, k_i is the frictional stress of the i^{th} grain, a is the crack length, c is the crack length plus slip band length, L_i is the distance from the free surface to grain boundary of the i^{th} grain preceding the slip band tip as shown in Figure 2.

The CTOD is given by

$$\phi_i = \frac{2k_j a}{\pi^2 A} \ln \frac{c}{a} + \sum_{i=j+1}^n \frac{(\tau_{i-1} - k_{i-1}) - (\tau_i - k_i)}{\pi^2 A} g(a; c, L_{i-1})$$

$$g(a; c, L) = L \ln \left| \frac{\sqrt{c^2 - L^2} + \sqrt{c^2 - a^2}}{\sqrt{c^2 - L^2} - \sqrt{c^2 - a^2}} \right| - a \ln \left| \frac{a\sqrt{c^2 - L^2} + L\sqrt{c^2 - a^2}}{a\sqrt{c^2 - L^2} - L\sqrt{c^2 - a^2}} \right| \quad (4)$$

$$A = G/2\pi(1-\nu) \text{ for edge dislocations}$$

$$A = G/2\pi \text{ for screw dislocations}$$

If the slip band is blocked by a grain boundary, equations (3) and (4) are modified slightly (Tryon, 1997).

Long crack growth model

The long crack growth is modeled using the Paris law representation of a surface crack in a semi-infinite body subjected to a constant stress cycle. If the final crack size is much greater than the initial crack size, Tryon and Cruse (1997) showed that

$$N_g = \frac{a_i^{1-n/2}}{C\Delta\sigma^n \beta^n \left(\frac{n}{2} - 1\right)} \quad (5)$$

where, N_g is the number of cycles needed for the crack to grow to failure, a_i is the initial crack size at the start of the long crack growth phase, $\Delta\sigma$ is the global stress range, β is the geometry constant ($1.12\sqrt{\pi}$), and C and n are based on material properties.

Modeling the Physical Microstructure

Consider a random array of grains as shown in Figure 3. A crack nucleates in the surface grain X_0 and then grows along the x axis as a semicircle through zones in which the effective material properties are uniform. After successful crack nucleation, the crack grows from grain X_0 into zone 1. In the example shown in Figure 3, zone 1 contains three grains. The effective material properties of zone 1 are defined as the average of the properties of the individual grains. As the crack grows, more grains are contained in each zone. As the crack becomes long, the effective material properties approach the bulk properties and long crack similitude is achieved.

Using the concepts of effective material properties, crack growth is modeled as two dimensional. Consider a cut along the x -axis (Section A-A in Figure 3). The fatigue damage is modeled as a crack growing through zones of varying size and varying effective material properties.

Monte Carlo Simulation Model

Consider a simple component such as a smooth round bar subjected to constant stress throughout. Monte Carlo simulation is used to predict the component fatigue life. The statistical characteristics of variables use in the Monte Carlo simulation have been discussed in detail in Tryon and Cruse (1995).

The basic flow of the Monte Carlo simulation is outlined as follows. A crack is nucleated in each surface grain of a component. An array of random grains such as Figure 3 is created in front of the nucleated crack and the crack goes through the small crack growth phase. At the end of the small crack growth phase, microstructural similitude is achieved and the crack goes thorough the long crack growth phase. The total life associated with each grain is the summation of the cycles in the crack nucleation, small crack growth and long crack growth phases. The life of the component is equal to the minimum total life of all of the grains. The details of the simulation are described in Tryon (1997).

The predictions of the individual crack nucleation, small crack

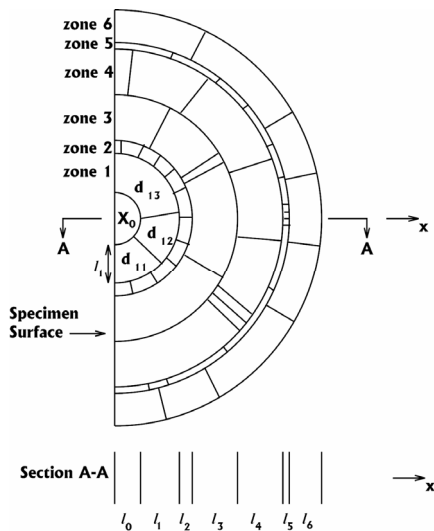


Figure 3: Array of random grains.

growth, and long crack growth simulations have been shown to correlate very favorably with experimental observations and are discussed elsewhere (Tryon and Cruse, 1997; Tryon and Cruse, 1998). In this section, we will discuss the prediction of the total fatigue life for a simple component.

The material used in the following microstructural simulations is a nickel alloy. The specifications for the material simulated are given in Table 1. This data was adapted from several investigations in the literature on fine grain Waspaloy (Abdul-Latif, 1996; Coles *et al*, 1978; Merrick, 1974).

Table 1: Specimen Parameters

Material Property	Value
Shear Modulus	11000000 psi
Poisson's Ratio	0.3
Small Crack Coefficient	0.01
Paris Law Exponent	3.1
Frictional Strength (k)	65000 psi
Grain Boundary SIF (K_C)	3400psi $\sqrt{\text{in}}$
Specific Fracture Energy (W_C)	340 lbs/in
Applied Stress ($\sigma_{\text{max}}, \sigma_{\text{min}}$)	$\sigma_{\text{max}} = 160000$ psi $\sigma_{\text{min}} = 0$ psi
Gage Area	0.188 in ²
Grain Size	0.000226 in.
Defect Size	0.0008 in

Simulation Results

The samples for the simulations are 500 smooth round bar components. Previous analysis showed that an ensemble of 500 simulations is large enough to observe the nature of the distribution of the failure parameters (1997). Of the 500 simulated components, 472 failed before the 10^{10} cycle test suspension. Of the 472 failures, 188 were due to defects, the others were due to transgranular crack nucleation.

The simulated data is used to determine the statistical distributions of various conditions at the location where the crack initiated including grain size, grain orientation, frictional strength, microstress and defect size.

Grain Size

Grain size is assumed to influence the fatigue life because a large grain has a large unobstructed slip distance that allows for a large number of dislocations to build-up. The large dislocation build-up causes an associated high energy, which leads to cracking of the grain. Figure 4 shows the grain size distribution of all of the grains in a typical smooth bar specimen. The average grain size for the example fine grain Waspaloy is 0.226 mils (0.000226 in.) with a coefficient of variation (COV) of 0.34 and a lognormal distribution. An axial fatigue test at 160 ksi of 500 specimens was simulated and 284 specimens failed by transgranular crack nucleation before the 10^{10} cycle test suspension. The grain that initiated the failure causing crack was identified, recorded and labeled "failure grain." Figure 4 compares the failure grain size distribution of the 284 failed specimens with the overall grain size distribution. The figure indicates that the failure grains have a size well into the upper tail of the overall grain size distribution. The average failure grains size was 0.649 mils, which is above the 99.9th percentile of all grains and 287% of the average grain size.

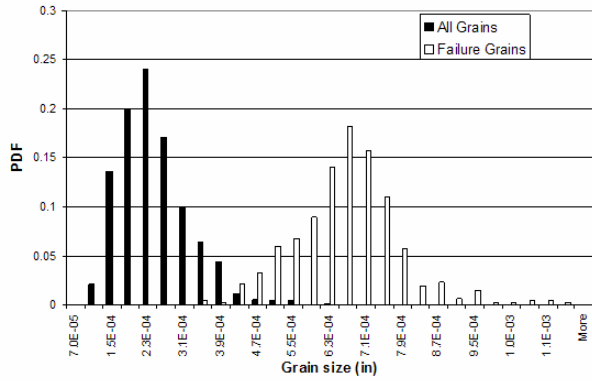


Figure 4: Grain size distribution of the grains that initiated failures in 284 specimens compared with the overall grain size distribution.

The smallest grain to cause failure in the 284 failed specimens was 0.316 mils, which is above the 88th percentile of all grains and 140% of the average grain size. The simulation predicts that the extremely large grains are governing the fatigue behavior. The COV of the failure grain size is 0.18 this is about half of the COV of the overall grain size distribution.

Grain Orientation

Grain orientation is assumed to influence the fatigue life because a sympathetically oriented grain allows a large resolved shear stress to easily move dislocations. The large dislocation build-up causes an associated high energy, which leads to cracking of the grain. However, nickel alloys have a face center cubic (fcc) crystalline structure with 12 active slip systems. Thus, at any grain orientation, there is a slip system that is nearly a sympathetic orientation. The model used to determine the slip orientation is represented as the reciprocal Schmid factor for fcc crystals. Figure 5 shows the grain orientation distribution for all of the grains in a typical smooth bar specimen. The figure shows that the minimum (most sympathetic) grain orientation is 2.0 which is in agreement with theory. The average grain orientation is 2.24. The upper limit can theoretically reach a value of 3.67.

Along with the failure grain size, the orientation of the failure grain was identified and recorded in the test simulations discussed

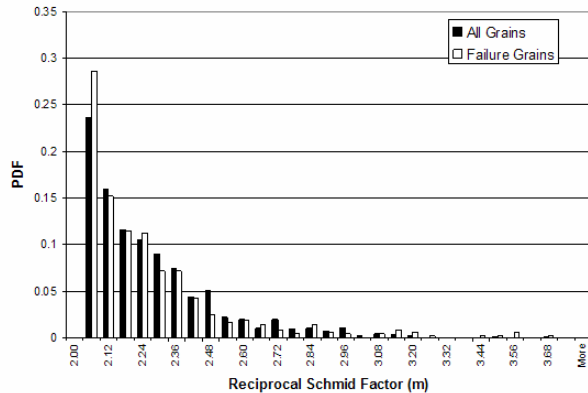


Figure 5: Grain orientation distribution of the grains that initiated failures at in 284 specimens compared with the overall grain orientation distribution.

above. Figure 5 compares the grain orientation distribution of all grains that compose the specimens with the grain orientation distribution of the grains that initiated failure at 160 ksi. It appears that the failure grains have an orientation slightly below the mean of the overall grain orientation distribution. The average failure grain orientation was 2.20 which is 98% of the overall average grain orientation. The most sympathetic orientation to cause failure in the 284 failed specimens was 2.021, which is near the minimum value of 2.0 for all grains. The most unsympathetic orientation to cause failure was 3.36, which is above the mean value for all grains. Although most of the grains that initiated failure were slightly more sympathetically oriented than the average grain, unlike the grain size, an extreme value grain orientation is not needed for fatigue initiation.

Local Microstructural Stress

Because each grain acts as an anisotropic single crystal, the actual loading on an individual grain is caused by the deformation of the surrounding grains, which are in turn loaded by the deformations of each of their surrounding grains. The microstress distribution is therefore a function of the anisotropic deformation of all of the grains that compose the structure.

The average microstructural stress is assumed to follow a normal distribution with a COV of 0.25. The COV of the local stress was based on Voronoi finite element models of nickel polycrystals (Zhao and Tryon, 2004). Figure 6 shows the microstructural stress distribution within all grains of a typical smooth bar specimen loaded to 160 ksi. Figure 6 compares the failure grain stress distribution of the 284 failed specimens with the overall grain stress distribution. This shows that the failure grains have a stress well into the upper tail of the overall grain stress distribution. The smallest microstress to cause failure in the 284 failed specimens is 192 ksi, which is above the 99.67th percentile of all grains. The largest microstress to cause failure is 302 ksi, which is above the 99.99th percentile. Based on the analysis, it can be deduced that large microstress is governing the fatigue behavior.

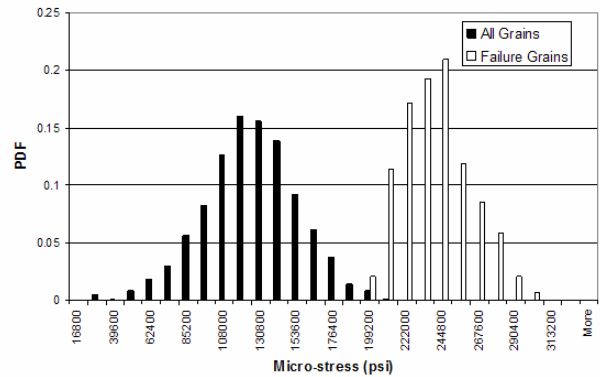


Figure 6: Microstress distribution of the grains that initiated failures at 160 ksi in 472 specimens compared with the overall microstress distribution.

Frictional Strength

The frictional strength is the stress that must be overcome for dislocations to move within a grain. The frictional strength can be thought of as the local yield strength. Because of the

crystallographic orientation of the grain, yielding takes place on well-defined planes in planar slip alloys. Experimental observations have shown that the frictional strength is nearly uniform across the grain (James and Morris, 1986).

There is little direct data available in the literature on the statistical distribution of the frictional strength. Although numerical determination of the grain to grain scatter in frictional strength has not been made, empirical observations provide some insight into the behavior of the scatter. Taira *et al.* (1978) experimentally observed the minimum cyclic stress for which slip bands formed in three different mean grain size microstructures of low-carbon steel. The applied stress was below the fatigue limit and slip bands formed in very few grains. They found that the minimum frictional strength is independent of mean grain size. The minimum frictional strength was nearly equal to the frictional strength predicted by the Petch relationship for the fatigue limit, expressed as

$$\sigma_f = k_f + \frac{K_m}{\sqrt{d}}$$

where σ_f is the fatigue limit, k_f is the frictional strength of the grains participating in fatigue, d is the mean grain size and K_m is the microscopic stress intensity factor.

Taira *et al.* used the Petch relationship for flow stress to determine the frictional strength for applied loads up to 5% plastic strain. As the load increased, more and more grains produced slip bands. By comparing the slip observed at high applied load to the slip observed at low applied load, one can get an indication of the scatter. At high applied load, many grains produce slip bands and the applied load may be thought of as the frictional strength of the nominal grain. At low applied load, only a few grains produce slip bands and this load may be thought of as the frictional strength of the weakest grain.

This method is not rigorous because the variation in the microstress is not taken into account. In addition, it is difficult to determine the shape of the distribution. A two parameter Weibull distribution was assumed and fitted to the data in Taira *et al.* The parameters of the Weibull distribution were determined by taking the applied stress of the 5% plastic strain test to be the frictional strength of the 50 percentile grain and the applied stress of the fatigue limit test was taken to be the frictional strength of the 1

percentile grain. This gave a normalized Weibull distribution with a shape factor $\beta_k = 3.7$ and a characteristic value $\eta_k = 1.12$ (mean value of 1 and a COV of 0.3). Tanaka *et al.* (1992) indicate that a two parameter Weibull distribution with COV between 0.3 and 0.7 can be used to describe the frictional strength.

Assuming a two parameter Weibull distribution for the frictional strength, Figure 7 shows the typical frictional strength distribution for all grains in a typical smooth round bar. Figure 7 also compares the failure grain frictional strength distribution of the 472 failed specimens at 160 ksi with the overall grain frictional strength distribution. This shows that the failure grains have a frictional strength slightly less the overall grain frictional strength distribution. The average failure grain's frictional strength is 52.9 ksi, which is 71% of the overall average frictional strength and near the 6th percentile of overall grains. The smallest frictional strength to cause failure in the 472 failed specimens is 8.73 ksi, which is below the 0.001th percentile of all grains. The largest frictional strength to cause failure was 111 ksi, which is below the 99.7th percentile. Therefore, this analysis indicates that grains with small frictional strengths tend to initiate the fatigue failure but the sensitivity is not as strong as grain size and microstress.

Defects

Depending on the relative elastic modulus, defect may or may not play a roll in fatigue crack nucleation in nickel superalloys. The higher the modulus, the more likely cracks will initiate at defects. A study of the effect of defects on fatigue life indicates that at high life, low strain, large subsurface defects are the dominant defect initiation sites (Boyd-Lee, 1999; Hyzak and Bernstein, 1982). Failure causing defects are thought to be among the largest in the specimen and therefore rare. At low life, high strain, small surface defects initiate failure. Apparently, at high applied load, the stress concentration at small defects is enough to initiate damage. The small defect initiates damage and because it is a surface defect, the damage grows more quickly to failure compared to damage growing from a small subsurface defect. At lower applied loads the stress concentration at the small defects is not sufficient to induce damage which gives the rare large internal defect sufficient time to grow to failure.

The important statistical parameters to be considered are the defect size and defect density. The simplest way to describe the size and density is to assume that the size and density are independent. A size distribution and a separate density distribution can then be established. For the nickel material of this study, the defect size was assumed to be log-normally distributed with a mean of 0.8 mils and a COV of 0.25. The defect density was assumed to be normally distributed with a mean of 40 defects/in² and a COV of 0.25. The probabilistic fatigue model randomly generates the number of defects in the specimen gage section based on the gage section area and the defect density distribution. The size of each of these defects is randomly generated by the defect size distribution.

Figure 8 shows the defect size distribution of a typical smooth bar specimen. An axial fatigue test at 160 ksi of 500 specimens was simulated and 472 specimens failed before the 10¹⁰ cycle test suspension. Of all the 472 failures, 188 were due to defects. The defects which caused failure were identified, recorded and labeled "failure defects." Figure 8 compares the failure defect size distribution of the 188 specimens that failed at defects with the

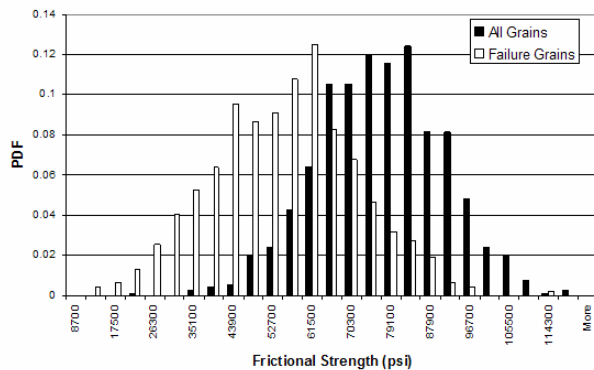


Figure 7: Frictional strength distribution of the grains that initiated failures at 160 ksi in 472 specimens compared with the overall distribution.

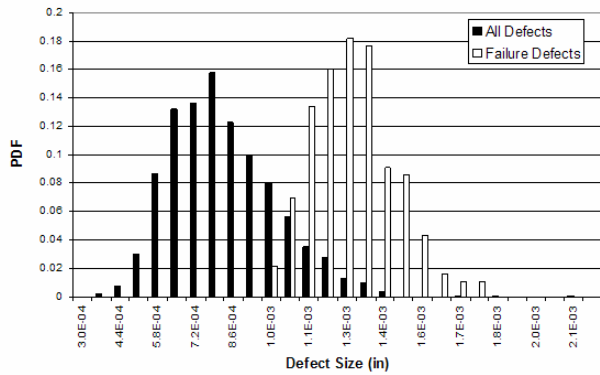


Figure 8: Defect size distribution of defects that caused failure in 188 specimens compared with overall the defect distribution.

overall defect size distribution. The average defect size to cause failure was 1.26 mils which is 160% of the mean size of all defects and above the 98.3th percentile of all defects. The COV of the failure defect distribution is 0.12 which is about half the COV of the distribution of all defects. The smallest defect to cause failure in the 188 specimens that failed due to defects was 0.933 mils, which is above the 77.6th percentile of all defects. It is obvious from the analysis that the larger defects govern fatigue life.

Experimental Fatigue Testing of Waspaloy

A used Waspaloy compressor disk was acquired by VEXTEC from the Air Force Research Laboratory and was used to assess the results from the fatigue simulation model. The average surface intercept size of the grains was 0.7 mils with a COV of 0.6. A typical microstructure is shown in Figure 9. The simulation model was developed and the predictions were made before the disk was made available. The microstructure of the disk was not the same as the microstructure of the model. The microstructure of the model was a fine grain size whereas the disk was a medium grain size. However, the relative predictions from the simulation should also be applicable to the medium grain size microstructure. Therefore, the disk was used as the basis for crack initiation testing and verification of the probabilistic microstructural fatigue simulation model.

During the testing, fatigue crack initiation and early propagation were studied using optical and electron microscopy, atomic force

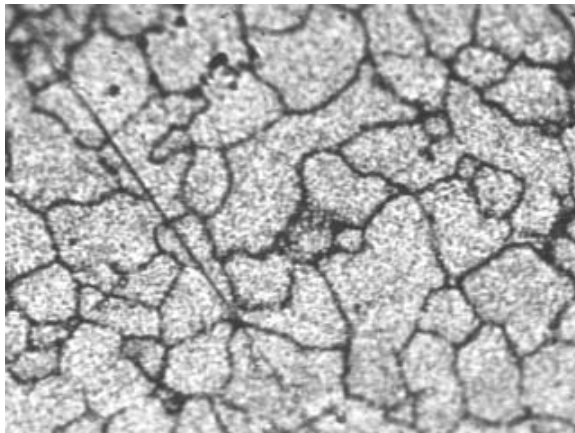


Figure 9: Typical microstructure of Waspaloy specimen.

microscopy and orientation imaging microscopy. A complete set of data as well as micrographs and other related quantitative information on grain orientations on the tested specimens were generated by the University of Utah. One of the objectives was to acquire detailed and quantitative information on Waspaloy crack initiation and the early crack growth (first 2-4 grain diameters) behavior at ambient temperature.

The testing generated experimental data that enabled an understanding of how a fatigue crack nucleates and what determines the site of crack nucleation. Additionally, the data helped to determine how the fatigue short crack growth was influenced by the crystallographic orientations of the grains.

Test Procedure

A bar specimen of 3.175 in. in length and 0.501 in. X 0.0305 in. in cross-section was used. The middle span (about 1 in.) of the specimen has a curved section of 1.08 in. in radius on two opposite sides to facilitate crack nucleation and replication. The cross-section at the middle of the specimen is 0.0305 in. X .254 in. The shoulder length is about 1.08 in. on either side of the curved section. The specimens were electrolytically polished and lightly etched such that the microstructure details were revealed in the replicas. These facilitated the tracing of the crack initiation location in replicas using the features as reference markers.

Fatigue tests were performed on a hydraulic 810 MTS, using the MTS TestStar II Fatigue Test software application. Inputs to the software included minimum and maximum force on the sample. The typical testing scheme was with a load ratio $R=0.1$ (where R is the minimum load of the cycle divided by the maximum load of the cycle). Cycles of fatigue testing were performed on the specimen, and the specimen was taken out either periodically or at set intervals for viewing under an Olympus PME 3 optical microscope with a Hitachi CCD camera for image capture. Cracks were usually formed after ample slip bands had appeared inside a grain in the specimen cross section where the stress range was the highest. Once cracks had been initiated and observed in the specimen, a record was kept of those cracks with optical micrographs. Once the crack had grown to sufficient size, testing was typically suspended with several cracks on each specimen.

Experimental Results

One of the specimens, tested at a maximum cyclic load of 116 ksi, had six crack nucleation sites that were studied. Figure 10 shows a typical crack initiation site. The crack was first noticed at 100 keycycles with a length of 1.7 mils. At 270 keycycles the test was suspended because several of the cracks were growing rapidly. The crack from Figure 10 was 10 mils at this time. The longest crack on the specimen had a surface length of 15 mils.

The 6 cracks were analyzed in detail by comparing the grains that were adjacent to the crack at initiation with a random sample of grains. Photo micrographs and orientation imaging microscopy (OIM) were used to determine the size and the orientations of the grains. Figure 11 shows the orientation regions for the crack of Figure 10. The loading direction is in the vertical direction. The first observable crack is marked on the photo micrographs by 2 vertical lines across the crack. Each region of differing orientation is indicated by a number. Many of the grains were twinned. For example regions 15, 16 and 25 are twins within the same grain.

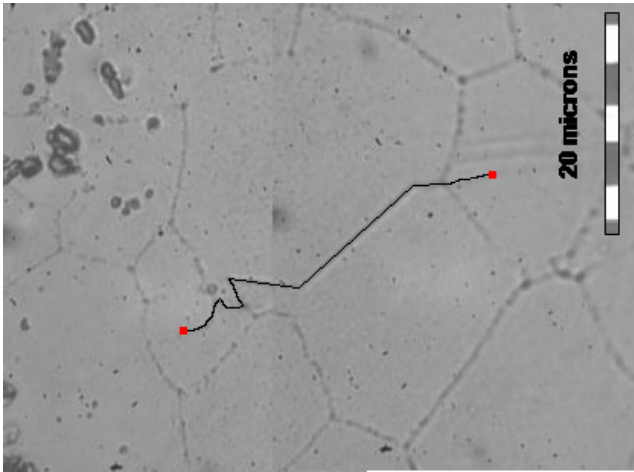


Figure 10: Typical crack nucleation site on the Waspaloy specimen. Dark line indicates the crack when the crack was first observed at 100 keycycles.

The grain size and grain orientation factors adjacent to the initial crack for each of the six cracks initiation sites on the specimen were measured and compared with an uncracked control area of 50 grains.

The grain size was defined by the average of the grain height and grain width measured at the specimen surface. The average grain size in the uncracked control area was 6.5 mils which was close to the overall average grain size measurement of 7 mils. The largest grain in the uncracked control area was 212% of the average grain size. The average grain orientation (reciprocal Schmid factor) in

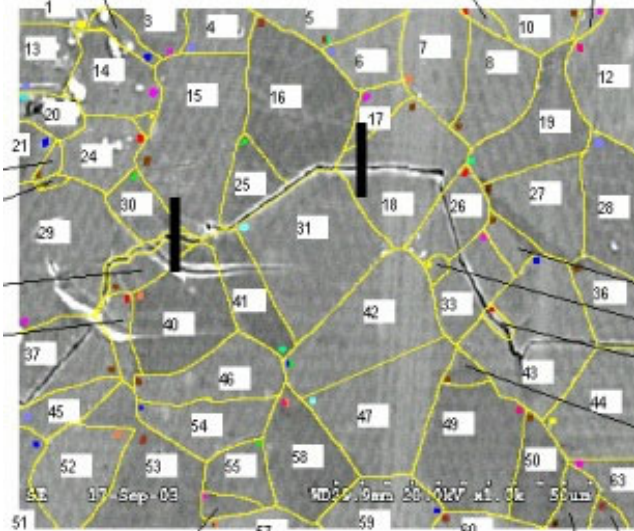


Figure 11: Orientation regions at the crack nucleation site. The crack nucleated between the two dark vertical lines.

the uncracked control area was 2.22 which is close to the overall average grain orientation of 2.24. The most unsympathetically oriented grain in the uncracked control area had an orientation of 3.59 was 162% of the average grain orientation and near the theoretical maximum grain orientation of 3.67.

Table 2 shows the comparison of the crack initiation sites with the uncracked control area. The maximum size of any grain adjacent to the initial crack was large; three sites had a maximum grain size larger than the control area. The fatigue simulation model predicted that the grain in which the crack initiated would be large, about 287% of the average grain size. Large grains were observed at the crack initiation sites for the test. These grains were about 227% of the average grain size. This is close to the predicted value. Notice also that the crack not only initiated at large grains but the cracks initiated at large grains surrounded by other large grains. The average grain size of the grains surrounding the crack initiation site was 157% of the overall average grain size. A region of many large grains was not observed in the uncracked control area. The test data confirms the simulation results that indicate that the crack will nucleate at a large grain.

The COV of the largest grain at the crack initiation site is 0.28 which is about half of the COV of the overall grain size distribution of 0.6. The fatigue simulation model predicted that COV of the failure grain size distribution would be about half of the overall grain size distribution.

Table 2 shows that the orientation (reciprocal Schmid factor) of the large grain at the crack initiation sites was similar to the average overall orientation of all grains. The average orientation of the large grain at the initiation site was 2.23 which is very close to the predicted orientation of 2.20. The orientation of all grains surrounding the crack initiation site was 2.19. This is very close to the average overall orientation of 2.22.

One of the cracks on the specimen (crack 6) nucleated at a defect. The crack initiation site is shown in Figure 12. The crack was 3.3 mils long when first noticed at 210 keycycles. The crack tips were at the two dark vertical lines in Figure 12. The crack had grown to 8.3 mils when the test was suspended at 270 keycycles. The defect size is 0.6 mils. However, the etch used to polish the surface makes the defects appear to be larger than they really are. Although defect measurements were not performed during the present study, an unpublished study performed by the United State Air Force Research Laboratory measured the statistical distribution of the defect size for another Waspaloy disk that should be representative of the defect population for the disk used in the present study (Caton and Rosenberger, 2004). They found the average defects size to be about 0.23 mils. Thus, the apparent size of the crack initiating defect is 260% of the average defect size. The fatigue simulations model predicted that the average size

Table 2: Comparison of the six crack initiation sites with the control area and the model predictions.

Factor	Random location	Crack 1	Crack 2	Crack 3	Crack 4	Crack 5	Crack 6	Average of 6 cracks	Simulation Prediction
Size of largest grain at each initiation site (% of overall average grain size)	212%	181%	338%	170%	187%	237%	249%	227%	287%
Average size of all grains at each initiation site (% of overall average grain size)	100%	119%	224%	148%	134%	149%	170%	157%	NA
Reciprocal Schmid factor of maximum size grain	2.22	2.22	2.18	2.22	2.12	2.38	2.28	2.23	2.20
Reciprocal Schmid factor of average orientation	2.22	2.20	2.17	2.25	2.16	2.22	2.16	2.19	NA

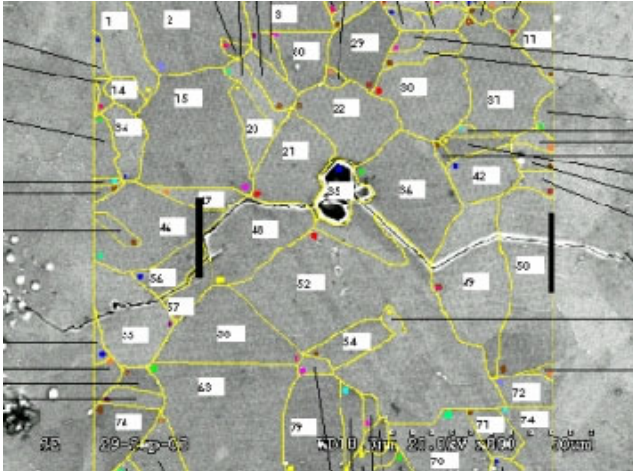


Figure 12 Orientation regions at the crack nucleation site. The crack is assumed to have nucleated at the defect. The crack tips were at the two dark vertical lines when the crack was first noticed.

of a crack initiation defect would be about 160% of the average defect size. Because the defect is actually smaller than it appears, the size of the crack initiating defect is similar to the prediction.

Summary

The probabilistic microstructural fatigue simulation software allows the user to predict statistical information on the values of the microstructural parameters associated with the crack initiating event. The laboratory test showed that large grains and nominal orientations were observed at the crack initiation site. This was predicted by the fatigue simulation model. The original hypothesis was that grains at the initiation site must have an extreme value of sympathetic orientation. The simulation model indicated this was not the case and the laboratory test confirmed this. Twelve slip systems are active in nickel alloys, thus a grain with a sympathetic orientation is not rare. One of the laboratory test crack sites included a defect that was much larger than the average defect size. The simulation predicted that large defect could initiate cracks. The probabilistic microstructural fatigue simulation model allows easy comparisons with available experimental data and prediction of the microstructural conditions sympathetic to fatigue crack initiation. This allows for the identification of the microstructural variables that need to be measured to determine the fatigue resistance and monitor fatigue damage progress. Once the microstructural state had been determined, the simulation model can be used to predict the statistical distribution of the residual useful life.

Acknowledgements

This paper was based on a study funded by DARPA contract DAAH01-02-C-R196 and United States Air Force Research Laboratory contract F33615-00-5209. The authors thank Drs. Leo Christodoulou, Jay Jira and Andrew Rosenberger for their support during this study.

References

Abdul-Latif, A. (1996), "Constitutive Equations for Cyclic Plasticity of Waspaloy," *International Journal of Plasticity*, Vol. 12, No 8, pp. 967-985.

Boyd-Lee A. D., (1999) "Fatigue Crack Growth Resistant Microstructures in Polycrystalline Ni-base Superalloys for Aeroengines," *International Journal of Fatigue*, Vol. 21, pp. 393-405.

Caton, M., Rosenberger, A, (2004) Private Communication.

Cowles B.A., Sims D.L., Warren J.R., (1978) "Evaluation of Cyclic Behavior of Aircraft Turbine Disk Alloys", Pratt &Whitney Report for: NASA CR-159409 FR10299.

Hyzak J. M., Bernstein, I. M., (1982) "The Effect of Defects on the Fatigue Crack Initiation Process in Two P/M Superalloys: Part 1. Fatigue Origins," *Met. Trans.*, Vol. 13A, pp. 33-43.

James, M. R., Morris, W. L., (1986) "The Effect of Microplastic Surface Deformation on the Growth of Small Cracks," *Small Fatigue Cracks*, Ed., R. O. Ritchie, J. Lankford, TMS, Warrendale, PA, pp. 167-189.

Merrick H.F., *Metallurgical Transactions*, (1974), "The Low Cycle Fatigue of Three Wrought Nickel-Base Alloys", Vol. 5, pp. 891-897.

Taira, S., Tanaka, K., Nakai, Y., (1978) "A Model of Crack Tip Slip Band Blocked by Grain Boundary," *Mech. Res. Comm.*, Vol. 5, No. 6, pp. 375-381.

Tanaka K., Kinefuchi, M., and Yokomaku, T., (1992) "Modelling of Statistical Characteristics of the Propagation of Small Fatigue Cracks," *Short Fatigue Cracks*, Eds. Miller, K. J., and de los Rios, E. R., ESIS 13, Mechanical Engineering Publications, London, pp. 351-368.

Tanaka, K., Mura, T., (1981)"A Dislocation Model for Fatigue Crack Initiation", *ASME J. Appl. Mech.*, Vol. 48, pp. 97-103.

Tryon, R. G., (1997) "Probabilistic Mesomechanical Fatigue Model", *NASA Technical Reports*, NASA/CR-97-202342.

Tryon, R. G., Cruse, T. A., (1998) "A Reliability-Based Model to Predict Scatter in Fatigue Crack Nucleation Life", *Fat. Frac. Eng. Mat. Str.*, Vol. 21, pp. 257-267.

Tryon, R. G., Cruse, T. A., (1997) "Probabilistic Mesomechanical Fatigue Crack Nucleation Model", *ASME J. Eng. Mat. Tech.*, Vol. 19, No. 1, pp. 65-70.

Tryon, R. G., Cruse, T. A., (1995) "Probabilistic Mesomechanical Fatigue Crack Initiation Model, Phase 1: Crack Nucleation", *ASME/JSME Pressure Vessel and Piping Conference*, Honolulu, HI, Published in PVP-95-MF2.

Zhao, Y., Tryon, R. G., (2004) "Automatic 3-D Simulation and Micro-Stress Distribution of Polycrystalline Metallic Materials," *Computer Methods in Applied Mechanics and Engineering*, Vol. 193, pp. 3919-3934.